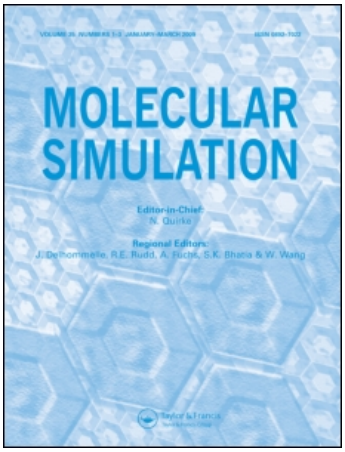

Molecular Simulation
Publication details, including instructions for authors and subscription information:
http://www.informaworld.com/smpp/title~content=t713644482

Molecular dynamics simulations for drug dosage form development: thermal and solubility characteristics for hot-melt extrusion

Martin Maus[a]; Karl G. Wagner[bc]; Andreas Kornherr[d]; Gerhard Zifferer[e]
[a] Department of Quality Operations, Boehringer Ingelheim Pharma GmbH & Co. KG, Biberach, Germany [b] Department of Pharmaceutical Technology, Institute of Pharmacy, University of Tuebingen, Tuebingen, Germany [c] Department of Pharmaceutical Research and Development, Boehringer Ingelheim Pharma GmbH & Co. KG, Biberach, Germany [d] Mondi Uncoated Fine Paper, Ulmerfeld-Hausmening, Austria [e] Department of Physical Chemistry, University of Vienna, Vienna, Austria

To cite this Article Maus, Martin , Wagner, Karl G. , Kornherr, Andreas and Zifferer, Gerhard(2008) 'Molecular dynamics simulations for drug dosage form development: thermal and solubility characteristics for hot-melt extrusion', Molecular Simulation, 34: 10, 1197 — 1207
To link to this Article: DOI: 10.1080/08927020802411695
URL: http://dx.doi.org/10.1080/08927020802411695

Molecular Simulation
Vol. 34, Nos. 10–15, September–December 2008, 1197–1207

Taylor & Francis
Taylor & Francis Group

Molecular dynamics simulations for drug dosage form development: thermal and solubility characteristics for hot-melt extrusion

Martin Maus[a]*, Karl G. Wagner[bc], Andreas Kornherr[d] and Gerhard Zifferer[e]

[a]*Department of Quality Operations, Boehringer Ingelheim Pharma GmbH & Co. KG, Biberach, Germany;* [b]*Department of Pharmaceutical Technology, Institute of Pharmacy, University of Tuebingen, Tuebingen, Germany;* [c]*Department of Pharmaceutical Research and Development, Boehringer Ingelheim Pharma GmbH & Co. KG, Biberach, Germany;* [d]*Mondi Uncoated Fine Paper, Ulmerfeld-Hausmening, Austria;* [e]*Department of Physical Chemistry, University of Vienna, Vienna, Austria*

(*Received 28 January 2008; final version received 12 August 2008*)

Properties of pharmaceutical drug polymer mixtures like miscibility, stability and drug release are determined by the interactions of active pharmaceutical ingredients (APIs) and excipients (e.g. plasticisers) with functional polymers. Molecular dynamics (MD) simulations (Materials Studio®, COMPASS force field) are used to predict the principal behaviour of such drug products, especially miscibility and glass transition temperature (T_g). Different mixtures containing APIs (theophylline or ibuprofen (IBU)) and water-soluble (triethyl citrate, (TEC)) or water-insoluble plasticiser (acetyl tributyl citrate (ATBC) or dibutyl sebacate (DBS)) dissolved/dispersed in a cationic polymethacrylate (EUDRAGIT® RS) were studied. Force field-based calculations of the cohesive energy densities of single constituents led to a qualitative approach according to Hanson describing the solid state of the mixture, while further calculations on the basis of the theory of free energy of mixing facilitated a semi-quantitative prediction. In the case of miscibility also calculation of T_g was possible via modelling specific volumes of amorphous cells at various temperatures. The simulated data correlated well with the experimental data obtained from differential scanning calorimetry (DSC) of drug products processed via hot-melt extrusion. Accordingly, the described method facilitates a good estimate of pharmaceutical polymer drug mixtures, thus decreasing product development time, as well as the consumption of active ingredients.

Keywords: drug dosage form; glass transition; plasticiser; polymer; solubility

1. Introduction

In the last decade, the use of molecular dynamics (MD) simulations has become more and more familiar to pharmaceutical developers, e.g. by checking on polymorphisms [1,2] and calculating properties of host–guest complexes [3,4]. Furthermore, MD simulations can assist dosage form development by predicting valuable physicochemical properties like viscosity of solutions [5], diffusivity [6] and water adsorption [7]. However, the above-mentioned parameters are often limited to 'small' systems either related to the molecular weight of the drug compound or the excipient employed. The aim of our study is, therefore, to find *in silico* test models using MD methods for polymers, excipients, drugs and mixtures thereof exceeding standard MD applications in complexity, and hence facilitates preformulation even at a stage where the drug compound or polymer are in an *in silico* stage of development. Also, the risk of unexpected physical or chemical incompatibilities (e.g. immiscibility) during the formulation process, which is time consuming and expensive [8], might be decreased. Fortunately, molecular simulation offers the possibility to calculate many relevant physical properties of the desired excipient and drug molecules, as well as of the polymer without the need of costly experiments.

In this respect, the *in silico* prediction of the thermodynamic mixing behaviour of different polymer–drug/excipient mixtures is of central interest. A common approach to cope with this problem is the calculation of the solubility parameters according to Hildebrand or Hansen [9–12], which is standard in the development of polymer mixtures [13]. The use of highly developed force fields as the basis of any MD simulation software enables the calculation of solubility parameters with an accuracy comparable with those measured experimentally by inverse gas chromatography [14], and an increasing number of other statistical quantitative property relationship between simulated and experimental values are established [15–18].

Focusing on polymer plasticiser blends, the glass transition temperature (T_g) is an important property in order to predict the formation of a solid solution. Homogeneous polymer plasticiser blends undergo a second-order-like phase transition at this temperature [19], passing from the

*Corresponding author. Email: martin.maus@boehringer-ingelheim.com

ISSN 0892-7022 print/ISSN 1029-0435 online

DOI: 10.1080/08927020802411695
http://www.informaworld.com

rubbery to glassy state with T_g decreasing with increasing plasticiser concentrations [20,21]. Throughout the literature, several approaches to determine the glass transition temperature of polymers via computer simulations are reported based on the change in various physical properties at T_g. One common approach is to determine the kink in a graph of the specific volume v versus temperature T [14,19,22–27], originating from the change in the thermal expansion coefficient. Other approaches also use the increase in potential energy [23–26] at T_g or the temperature dependence of the mean square displacement of polymer chains below and above T_g [26,28]. Normally, all these methods lead to a good prediction of T_g values for *pure* polymers.

Simulations of pharmaceutical relevant *mixtures* of polymer/excipient/drug blends, however, are scarce. Momany and Willett [25] investigated the dependence of T_g of maltodecaose on its hydration (water is known to act as a plasticiser for carbohydrates) and Yoshioka et al. [29] probed T_g values of freeze-dried dextran cakes. Quite recently, we studied the T_g dependence of an ammonio methacrylate copolymer (EUDRAGIT® RS) as a function of its triethyl citrate (TEC) content [27], which was in good agreement when compared with experimental data.

In this follow-up study, we want to examine the miscibility and the impact on the drug dosage form in respect of T_g from systems including EUDRAGIT RS (a cationic ammonio methacrylate copolymer, type B), three common plasticisers (TEC, acetyl tributyl citrate (ATBC) and dibutyl sebacate (DBS)) and two active ingredients: ibuprofen (IBU) (likely plasticising impact on EUDRAGIT RS [30]) and theophylline (unlikely plasticising influence on EUDRAGIT RS [31,32–34]).

The aim is to assist the developer in the two pivotal development questions of a hot-melt extruded dosage form.

(1) What is the best polymer plasticiser mixture to obtain the lowest possible processing temperature for the extrusion process? A problem that is, of course, closely linked to a low value for T_g.
(2) What is the extent of the drug compound's solubility in the respective polymer plasticiser blend? The solubility should be rather high for the purpose of forming a solid solution to improve active pharmaceutical ingredient (API) solubility. And in contrast should be very low in case drug dispersion is intended to be formed to extend the API release from the polymer matrix.

In order to compare the simulated values with the hot-melt extrusion process, the feasible blends are produced through hot-melt extrusion, performed on a laboratory-scale ram extruder. Employing EUDRAGIT RS as a thermal polymer, which is known to form multiple-unit controlled-release matrix particles [20,34–36], the purpose in respect of question 2 was to distinguish a system of low solubility for the drug compound.

2. Materials and methods

All different substances used in this study are visualised in Figure 1 (all chemical structures are conformational, not optimised due to a better visibility).

2.1 Materials

TEC was purchased from Merck KGaA (Darmstadt, Germany). The other substances were kindly donated by various manufactures: EUDRAGIT RS 100 by Röhm GmbH (Darmstadt, Germany), ATBC by Jungbunzlauer Ladenburg GmbH (Ladenburg, Germany), DBS by Morflex Inc. (Greensboro, NC, USA), IBU by Knoll Pharmaceuticals (Nottingham, UK) and theophylline anhydrous powder by BASF AG (Ludwigshafen, Germany).

2.2 Numerical methods

2.2.1 Calculation of solubility parameters

In order to calculate the solubility of both plasticiser and drug molecules within a given polymer matrix, it is necessary to compute the so-called cohesive energy E_{coh}. This energy is a measure of the intermolecular forces (both electrostatic and dispersive) acting between the molecules of a specific substance. Accordingly, E_{coh} corresponds to the experimental value of the internal heat of vaporisation ΔH_{vap} (with R being the real gas constant) [10]

$$E_{coh} = \Delta H_{vap} - RT. \quad (1)$$

In a computer simulation, the energy (and force) between different molecules is directly accessible from the force field. Therefore, it is possible to compute E_{coh} directly and to transform it into the Hildebrand solubility parameter δ [10] according to

$$\delta = \sqrt{\frac{E_{coh}}{V}}, \quad (2)$$

where V is the volume of the phase from which E_{coh} is calculated.

For this numerical procedure, cubic simulation boxes (with periodic boundary conditions in all directions) containing either four polymer chains consisting of 62 monomer units each or 60 plasticiser/drug molecules are constructed. Dependent on the type of plasticiser, the cubic box size has a side length of *ca.* 4 nm (Figure 2). For each type of molecule, 10 independently generated simulation boxes are minimised with respect to the total energy. Out of those, the lowest energy system is further relaxed for

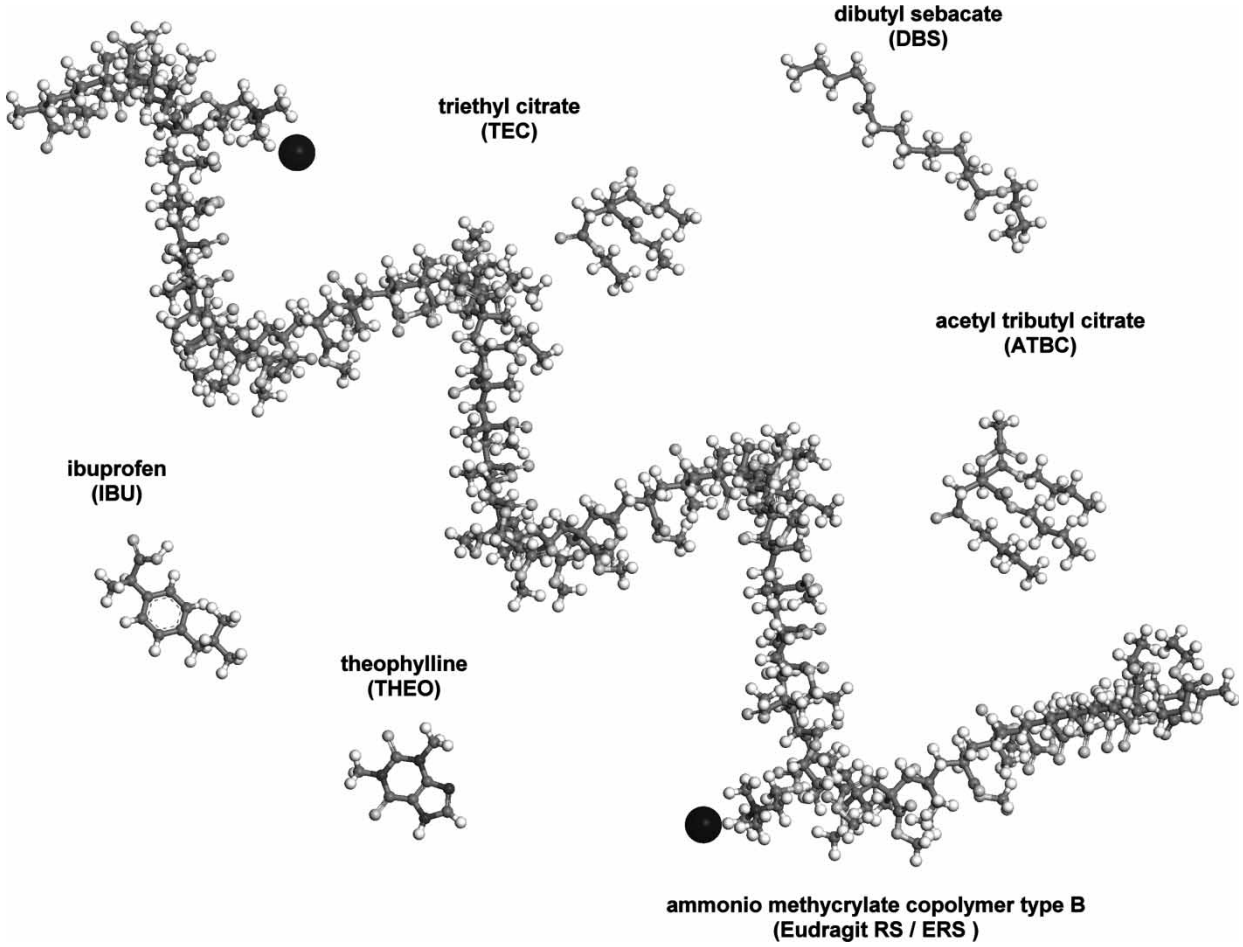

Figure 1. Visualisation of EUDRAGIT® RS polymer chain consisting of 64 monomers and all other molecules (both plasticisers and drugs) used in this study. The chlorine anion is depicted larger for better visibility; the different grades of grey in this and the following figures correspond to different atom types with white reserved for hydrogen, light grey for oxygen, grey for carbon and black for nitrogen or chlorine. All the graphical displays of molecules were generated with the Materials Visualizer (from Accelrys Inc.).

2 ns under *NPT* conditions at ambient conditions, i.e. at constant pressure (10^5 Pa) and constant temperature (298 K) to obtain a well-relaxed start structure with the correct density using the Anderson thermostat and barostat [37], with a time step of 1 fs. Afterwards, a 200 ps run at constant volume and constant temperature (i.e., NVT conditions) is carried out – 100 ps for equilibration and 100 ps for data sampling. Thus, the cohesive energy is averaged over this latter period and the corresponding cohesive energy density E_{coh}/V is calculated by dividing it through the volume of the simulation cell.

During minimisation as well as during the MD runs, energy summation is performed in direct space making use of a group-based cut-off for non-bond interactions. Strictly speaking, a cut-off distance of 1.25 nm with a spline switching function is applied for the Coulomb and van der Waals interactions (the latter being expressed by a 6–9 Lennard-Jones potential) using charge groups to prevent dipoles from being artificially split when one of the atoms is inside and another outside a (atom-based) cut-off.

For the whole simulation procedure, the software package MS Modeling 3.0 (from Accelrys Inc., San Diego, CA, USA) was applied using the Amorphous Cell tool for construction of the amorphous phase and Discover as the MD code. Atomic charges and interactions between atoms and molecules were accounted for by the use of the COMPASS force field [38–41], which is highly optimised for the simulation of condensed phases.

2.2.2 Determination of the specific volume as a function of temperature

The numerical procedure is very similar to the method briefly described in Section 2.2.1 (see also [27]). However, now several independent starting structures (generally three to five, to average the obtained final specific volumes to decrease scatter) of the corresponding system are chosen and relaxed for 2 ns under NPT conditions at a temperature of approximately 100 K higher than the supposed glass transition temperature. Afterwards, a

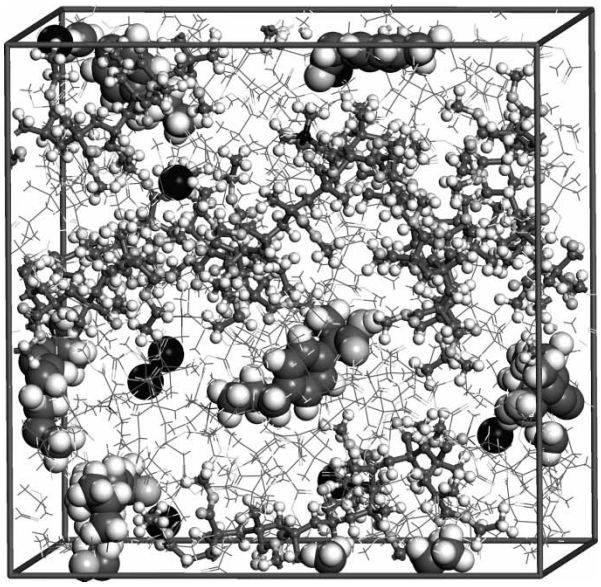

Figure 2. Simulation box (3.7 × 3.7 × 3.7 nm) with periodic boundaries showing four EUDRAGIT RS polymer chains and six IBU molecules after a relaxation time of 2 ns at 430 K. One polymer chain and all IBU molecules are visualised in ball-and-stick style to demonstrate the size of the box, as well as the distribution of the drug molecules.

'cooling process' is initiated by lowering the temperature stepwise by 10 K until a temperature ≈100 K lower than T_g is reached. At each temperature, 200 ps NPT ensemble dynamics is carried out – 150 ps for equilibration and 50 ps for data sampling (i.e. averaging the specific volume v over this period) using the final configuration of this run as the starting structure for dynamics at the next (10 K lower) temperature.

2.3 Experimental methods

2.3.1 Hot-melt extrusion

According to the aim of the study, the mixtures of the polymer and its plasticising agents were produced by hot-melt extrusion at 140°C. The ram extruder, assembled by an in-house precision mechanic shop, consists of a massive brass cylinder with a 1200 W heat source connected to a self-adapting power controller KS40-1 (PMA Prozess-und Maschinen-Automation GmbH, Kassel, Germany) equipped with a PT100 sensor. The barrel diameter is 10.0 mm and the length 280 mm. By connecting a material testing machine DO-FB0.5TS (Zwick GmbH & Co, Ulm, Germany) to the plunger, it was possible to control and measure the force and velocity used for the extrusion of the hot melts through the orifice. The material testing machine was controlled by the utilisation of programmable logic arrays included in the software testXpert ver. 2.02 (Zwick GmbH & Co, Ulm, Germany).

About 10 g of the physical mixture, containing the polymer and the respective plasticising substance at quantities from 0 to 25.5% (w/w), were prepared. These mixtures were manually poured into the ram extruder and equilibrated for 10 min at 140°C. The stability of the polymer under the chosen conditions has previously been analysed by thermogravimetric analysis (TGA) measurements [35,42]. All mixtures were extruded three times at a plunger velocity of 15 mm/min through a 2.0 mm orifice.

2.3.2 Differential scanning calorimetry (DSC) measurements

DSC measurements were performed for the experimental determination of the glass transition temperature T_g. The mean value of the onset and endset temperatures of the transition was calculated, according to DIN 53 765 A20. A Mettler TA 8000 calorimeter with a TAS 811 system and a DSC 820 measuring cell (Mettler-Toledo GmbH, Giessen, Germany) was used. Samples containing 20 mg polymer, including the respective plasticising substance, were accurately weighted and sealed in perforated 40 μl Al pans and further analysed under a dry nitrogen purge at a flow rate of 50 ml/min.

3. Results and discussion

This section is divided into three parts:

- First, we will discuss the determination of solubility parameters in order to predict and explain polymer–plasticiser/drug miscibility. It is very important – from both a theoretical and experimental point of view – to ensure that two components are able to build a stable homogeneous mixture.
- Second, we will apply this knowledge to decide which of the possible polymer–plasticiser/drug systems are suitable for the calculation of T_g.
- In the third part, the calculated T_g values will be compared with experimental values.

3.1 Numerical determination of solubility properties

A computational method in combination with a suitable force field provides an advantage, in contrast to the commonly used group number systems [9,43] for calculating the solubility parameters according to Hildebrand [10] and Hansen [11]. Recent comparisons of simulated solubility parameters with those measured using reverse gas chromatography and other experimental methods [44] proved the accurateness of the simulated values.

All plasticisers used in this study are commonly used for the application of polymer coatings as well as for matrix systems [31–33,45–47]. TEC is the standard

plasticiser for EUDRAGIT RS with a maximum water solubility of 5%, underlining its hydrophilic character. ATBC was chosen due to its structural similarity compared with TEC, but with an increased lipophilic character. The third plasticiser, the double butylated decanedicarboxy acid (DBS), has a similar lipophilic character as ATBC, but the different molecular structure allows for an additional testing of our computational method.

IBU as a non-steroidal anti-inflammatory is reported to have plasticising properties in combination with EUDRAGIT RS [30], thus representing a model drug with severe interactions with the polymer matrix. Its aromatic molecular structure presents a further change in the geometry as well as in the hydrophilic–lipophilic character. By contrast, the anti-asthmatic methylxanthine theophylline has proved its inertness within formulations containing EUDRAGIT RS [31–34], and was therefore chosen as the second active ingredient in our study.

The physical states of the substances modelled differ at 298.15 K: DSC measurements (see also Section 3.3.2) show that polymer EUDRAGIT RS is amorphous without crystalline sections. By contrast, the plasticisers TEC, ATBC and DBS are fluids. Furthermore, the drugs IBU and theophylline are crystalline, with IBU melting within the hot-melt extrusion process while theophylline stays solid. These differences were taken into account for the calculation of the solubility parameters: using crystallographic data from the Cambridge Structural Database, it was possible to calculate the solubility parameters of both these crystalline drugs and the corresponding amorphous (i.e. molten) state.

3.1.1 *Hildebrand solubility parameters*

The Hildebrand solubility parameters calculated within the MD simulation are presented in Table 1. As expected, crystalline drugs have the highest cohesive energy density with the Hildebrand parameter δ (see Equation (2)), reading 31.64 $(J/cm^3)^{0.5}$ for IBU and 51.43 $(J/cm^3)^{0.5}$ for theophylline. By contrast, amorphous substances show a reduced energy density due to the absence of the heat of crystallisation. With δ reading 17.43 $(J/cm^3)^{0.5}$, the pure polymer has the lowest solubility parameter. The plasticisers and amorphous IBU are in the same range up to a maximum of 20.95 $(J/cm^3)^{0.5}$ for IBU.

3.1.2 *Hansen solubility parameters*

Hansen [11] divided the Hildebrand solubility parameter δ into contributions from the non-polar van der Waals dispersion forces δ_d, the polar (electrostatic) interactions δ_p and the hydrogen bonding interactions δ_h

$$\delta^2 = \delta_d^2 + \delta_p^2 + \delta_h^2. \tag{3}$$

In most modern force fields like COMPASS, however, hydrogen bonding interactions are incorporated into the polar interactions; therefore, discrimination between δ_p and δ_h cannot be made. Accordingly, in our calculations, these parameters are combined to δ_e

$$\delta_e = \sqrt{\delta_p^2 + \delta_h^2}. \tag{4}$$

The Hansen solubility parameters that were calculated according to Equation 4 are presented in Table 1. With δ_d values of *ca.* 17–19 $(J/cm^3)^{0.5}$, all plasticising molecules were within a narrow range; only the polymer seemed to have a reduced dispersive solubility parameter value reading 13.13 $(J/cm^3)^{0.5}$. A better discrimination was possible by comparison of the different values of the electrostatic interaction parameter δ_e: with a δ_e value of 11.32 $(J/cm^3)^{0.5}$, the pure polymer was in the same range, compared with amorphous IBU (11.89 $(J/cm^3)^{0.5}$) and the hydrophilic plasticiser TEC (8.62 $(J/cm^3)^{0.5}$), thus indicating an excellent miscibility. By contrast, both the values of DBS (3.29 $(J/cm^3)^{0.5}$) and ATBC (4.57 $(J/cm^3)^{0.5}$) showed an extended lipophilic character.

Extremely high values, however, can be observed when considering the crystalline state of the drugs theophylline and IBU with δ_e readings of 45.85 $(J/cm^3)^{0.5}$ and 26.53 $(J/cm^3)^{0.5}$, respectively. In addition, even the – only

Table 1. Overview of densities, molar volumes and solubility parameters calculated via MD simulations.

	ρ (g/cm^3)	ν_M (cm^3)	δ $(J/cm^3)^{0.5}$	δ_e $(J/cm^3)^{0.5}$	δ_d $(J/cm^3)^{0.5}$
TEC	1.114	248.6	20.70	8.62	18.81
ATBC	1.039	387.5	17.96	4.57	17.37
DBS	0.910	345.4	17.63	3.29	17.32
IBU (amorphous)	0.977	211.2	20.95	11.89	17.25
IBU (crystalline)	1.092	188.9	31.64	26.53	17.23
THEO (amorphous)	1.350	133.5	29.48	16.99	24.10
THEO (crystalline)	1.493	120.7	51.43	45.85	23.29
ERS	1.028	6250.1	17.34	11.32	13.13

ρ (g/cm^3), density; ν_M (cm^3), molar volume; δ $(J/cm^3)^{0.5}$, overall Hildebrand solubility parameter; δ_e $(J/cm^3)^{0.5}$, solubility parameter representing the electrostatic interactions, according to Equation 4; δ_d $(J/cm^3)^{0.5}$, solubility parameter representing the dispersive interactions, according to Hansen.

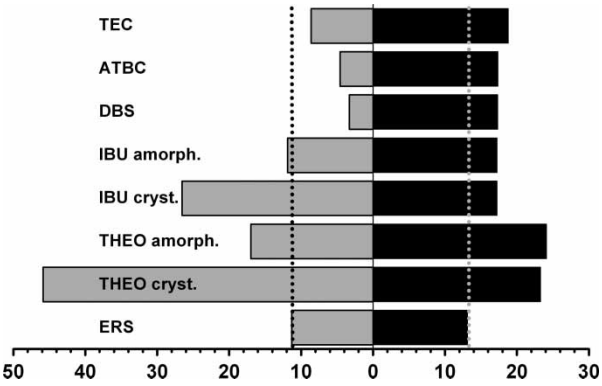

Figure 3. Visualisation of the dispersive δ_d (right-hand side, black) and the electrostatic δ_e (left-hand side, grey) solubility parameters, according to Hansen, with the upright dashed lines marking the values of the pure EUDRAGIT RS polymer.

hypothetical – amorphous state of theophylline showed a δ_e value of 16.99 $(J/cm^3)^{0.5}$ and a δ_d parameter value of (24.10 $(J/cm^3)^{0.5}$. Therefore, no miscibility of this drug with the polymer could be expected. For ease of comparison of the different δ_e and δ_d values, a graphical representation is given in Figure 3.

3.1.3 Flory–Huggins interaction parameter

The qualitative considerations of the previous section regarding the solubility of plasticisers/drug/polymer blends can be transferred to a quantitative prediction of miscibility by calculation of the Flory–Huggins interaction parameter χ [48]

$$\chi = \frac{V_{m1}\cdot(\delta_1 - \delta_2)^2}{R\cdot T}, \tag{5}$$

V_{m1}, molar volume of plasticising substance; δ_1, solubility parameter of plasticiser; δ_2, solubility parameter of polymer; R, 8.314472 J/(mol·K) (real gas constant); T, 298.15 K (absolute temperature).

An interaction parameter of zero describes an ideal solute–solvent system where the energetic interactions of two different molecules within a solution are equal to the interactions within the pure substance. The higher the value of χ the more dissimilar are the two substances, and therefore will not easily dissolve each other.

The calculation of this interaction parameter of different substances and the polymer displayed the differences as well as similarities of the studied blends (Table 2). For all classic plasticisers, the Flory–Huggins parameter χ was equal to or less than 1.132 when mixed with the polymer. For the crystalline drugs IBU and theophylline, χ would read 56.6 and 15.5, respectively, whereas the corresponding amorphous states show an extreme decrease in χ reading 1.1 and 7.9.

3.1.4 Gibbs free enthalpy change of mixing

The Gibbs energy of mixing ΔG_m [48] describes the overall thermodynamic benefit of generating a polymer–plasticiser mixture. Mixing of two substances only occurs in the case of negative values of ΔG_m. As a molecular solution of the plasticiser in the polymer matrix is an indispensable requirement for its plasticising properties, the possibility to calculate the value of ΔG_m prior to the specific experiment is extremely helpful in practice.

$$\Delta G_m = k\cdot T\cdot\left(\frac{N}{V_{m1}}\cdot v_1\cdot\ln v_1 + \frac{N}{V_{m2}}\cdot v_2\cdot\ln v_2 + \chi\cdot\frac{N}{V_{m1}}\cdot v_1\cdot v_2\right), \tag{6}$$

k, 1.38E·10^{-23} J/K (Boltzmann constant); T, 298.15 K (absolute temperature); N, 6.02E·10^{23} mol^{-1} (Avogadro constant); V_{m1}, molar volume of plasticising substance; V_{m2}, molar volume of polymer chain; v_1, 0.1 (volume fraction of plasticiser); v_2, 0.9 (volume fraction of polymer).

In Table 2, the ΔG_m values calculated according to Equation (6) for different polymer–plasticiser systems with a typical value for the plasticiser volume fraction of 10% are presented. As expected from the solubility parameters, these values are positive for the crystalline drugs and even for the hypothetical amorphous state of theophylline. Therefore, further simulations (and experiments) considering the plasticising properties of theophylline made no sense.

3.2 Simulation of plasticising properties

The glass transition temperatures of all substances that show a possible molecular miscibility with the polymer matrix were simulated. As described in the numerical section, a previously reported MD method [27] was applied.

Table 2. Calculated Flory–Huggins parameter χ and free enthalpy of mixing ΔG_m of 10% excipient with 90% polymer at 298 K.

	TEC	ATBC	DBS	IBU (amorphous)	IBU (crystalline)	THEO (amorphous)	THEO (crystalline)
χ	1.132	0.060	0.012	1.111	15.582	7.939	56.584
ΔG_m (J/cm^3)	− 1.318	− 1.476	− 1.682	− 1.566	15.343	9.965	99.846

3.2.1 *Different polymer/TEC solid-state solutions*

The first check of our improved model (four instead of eight polymer chains, but with a doubled chain length) for the MD simulations was a recalculation of T_g of the previously simulated [27] polymer–TEC systems. Again, a cooling of the new model of the pure polymer from 480 to 250 K in 10 K steps showed a clearly visible kink in the specific volume v versus temperature T diagram (Figure 4(a)), thus indicating a second-order-like phase transition from the rubbery to glassy state. The glass transition temperature (354 K) was indicated by the interception of two linear regression lines from the rubbery and glassy phase.

Analogous to the previous work [27], mixed systems containing four long polymer chains plus 6 or 12 TEC molecules per simulation box were constructed and the corresponding T_g values were determined (Figure 4(b), (c)): 332 K for the 6 TEC system and 308 K for 12 TEC system. Accordingly, the improved new model for the MD simulation of the TEC containing EUDRAGIT RS systems showed a nearly perfect linear correlation of a decreasing value of T_g at an increasing plasticiser concentration (Figure 5).

Although some deviation from experimental DSC data still occurred, the comparison with the previously reported [27] short-chain system (dotted line in Figure 5) clearly highlights the improvement of doubling the polymer chain length in the new model used in this work.

3.2.2 *Further solid polymer–plasticiser solutions*

Due to the good reproducibility of calculated and experimental T_g values of the plasticiser TEC, the more lipophilic plasticisers ATBC and DBS as well as the model drug IBU were also tested. Amorphous cells containing four polymer chains and six molecules of either ATBC, DBS or IBU were constructed and the corresponding T_g values were determined by analysing the kink in the v versus T diagrams (Figure 6).

All data points within the simulated temperature range of ATBC were included for the subsequent analysis. Due to the distinct kink in the v versus T graphs, it was easy to separate them into two parts (a rubbery and a glassy part) and fitting them to a straight line by linear regression (Figure 6(a)). By contrast, data points of both DBS and IBU showed a larger temperature interval where the glass transition seems to take place. This was indicated by larger deviations from the linear regression lines in the rubbery as well as in the glassy state. Accordingly, some values in this region without a clear defined physical state (rubbery or glassy) have been left out for analysis (Figure 6(b),(c)).

In Table 3, the calculated and the DSC measured glass transition temperatures of all simulated systems are presented. As expected, simulated T_g values were always higher than the experimental values due to the high cooling rate in a computer experiment (i.e. in an *in silico* experiment one could regard the system as being 'shock frozen'). However, the discrepancies were only 4–11%, thus indicating the reliability of the presented computational method.

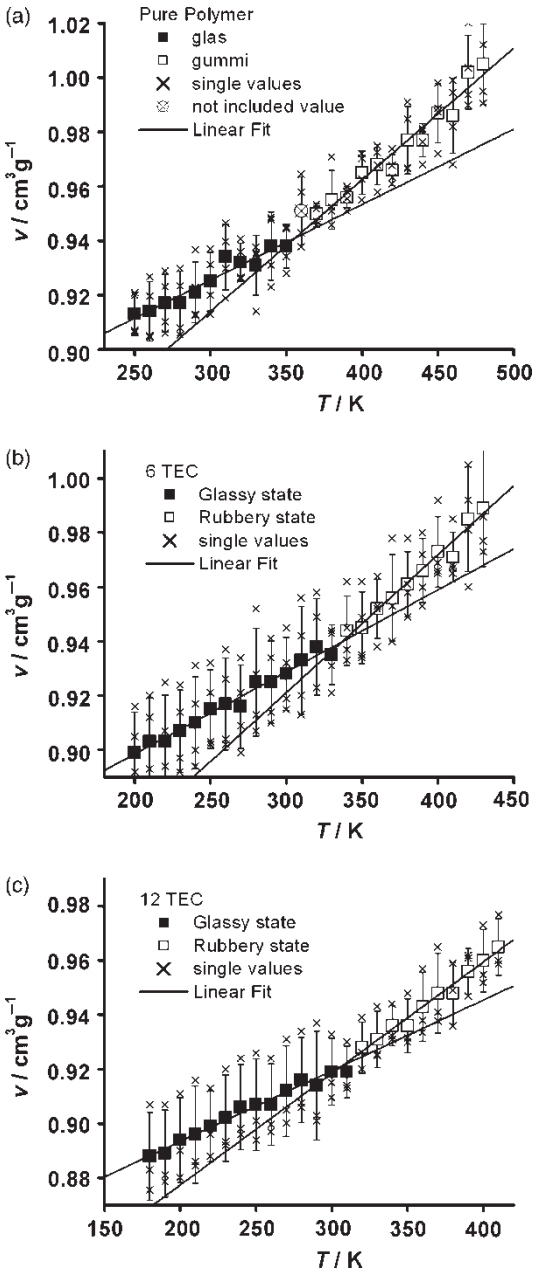

Figure 4. Plot of the computed specific volume v of (a) pure EUDRAGIT RS polymer, (b) EUDRAGIT RS polymer and 6 TEC as well as (c) 12 TEC molecules per simulation box versus temperature T of the system. The intersection point of the two lines resulting from a linear regression of the data points corresponding to the glassy (■) and rubbery (□) states determines the simulated T_g values (Table 3). All values are means of the specific volumes at the specified temperature of at least three independent systems; printed error bars represent the SD and circles represent values not used in the analysis.

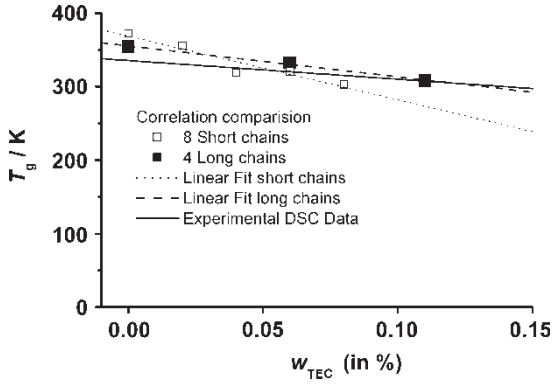

Figure 5. Comparison of the dependence of the glass transition temperature T_g on the TEC weight proportion w_{TEC} determined by the new MD model (filled symbols, dashed line), the MD model used in our previous communication (open symbols, dotted line) and experimental (solid line) DSC values. All lines result from a linear regression of the data points.

3.3 Experimental check of the plasticising properties

3.3.1 Production of solid solutions using a hot-melt ram extruder

All physical mixtures were extruded at the conditions stated in the experimental section. By subsequently extruding the mixtures three times, enough shear was applied to achieve well-distributed solid solutions of the plasticisers within the polymer matrix. A comparison of the development of the force effect during the extrusion cycles showed a reduction in the force effect at each step. This trend clearly indicated that the homogeneity increased through the multiple ram extrusion. Furthermore, all three plasticisers, TEC, ATBC and DBS showed either extreme stickiness, or a too soft consistency of the extruded polymer strands at levels higher than 25.5%. Therefore, a plasticiser fraction w of 25.5% (m/m) indicated the endpoint in the application range.

The crystalline drug IBU melts at 76°C, so the applied extrusion temperature allowed the incorporation of molten drug into the polymer matrix. Therefore, IBU could be homogeneously dissolved up to the values of w reading 20% (due to the high stickiness, no higher solid-state solutions could be produced).

By contrast, theophylline is melting at 270°C, so this drug remained crystalline during the entire hot-melt extrusion process and was only suspended in the polymer matrix. The compositions and glass transition temperatures of all samples produced by hot-melt extrusion are shown in Table 4.

3.3.2 Thermal analysis of the extrudates

The subsequent DSC measurements of the produced polymer–TEC, polymer–ATBC and polymer–DBS extrudates, up to a weight percentage of 19%, showed a clearly visible, strictly amorphous step when the heat flow was plotted against the reference temperature T. A representative DSC plot of the transition of the pure polymer as well as a polymer–TEC extrudate at 17% is shown in Figure 7.

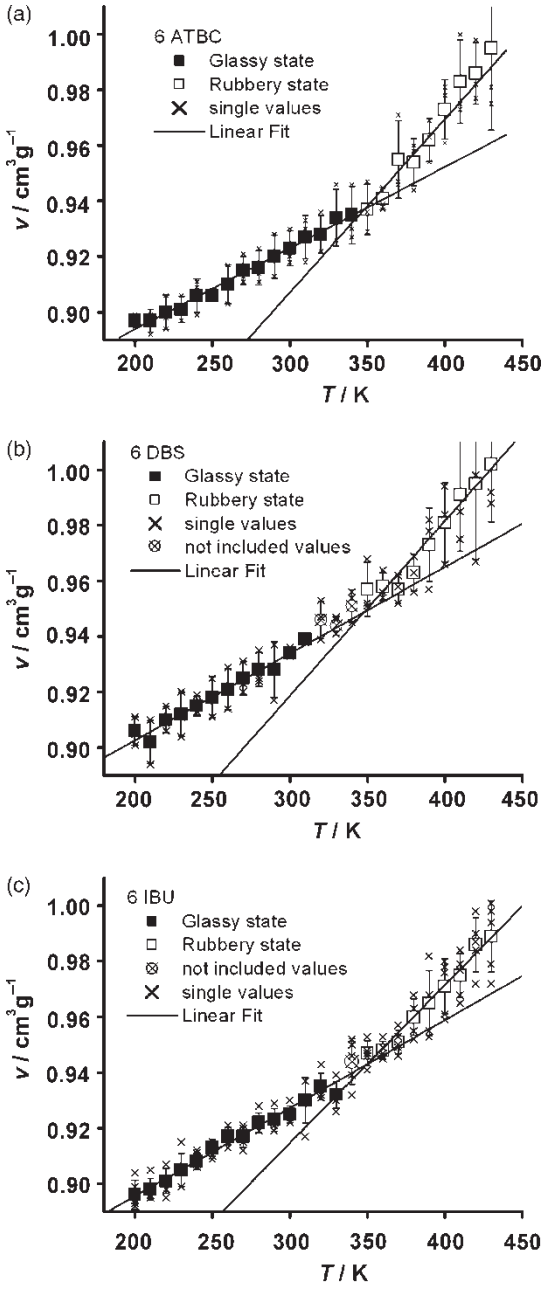

Figure 6. Plot of the computed specific volume v versus temperature T of three different polymer–plasticiser systems, each containing four polymer chains and (a) six ATBC, (b) six DBS, and (c) six IBU molecules per simulation box. Symbols and determination of T_g are as in the legend of Figure 4 (values can be found in Table 3).

Table 3. Overview of extrapolated experimental and calculated T_g values in Kelvin of the different polymer/plasticiser systems with n symbolising the number of plasticiser molecules per simulation box.

	ERS		TEC		IBU		DBS		ATBC	
n	DSC	MD	DSC	MD	DSC	MD	DSC	MD	DSC	MD
0	336.7	354								
6			320.2	332	328.5	349	315.9	348	316.3	353
12			306.5	308						

As it was reported earlier for other polymer/plasticiser blends [27,30,34,42,45], the measured T_g values of the extrudates exhibited a linear dependence on to the mass fraction w of plasticiser in the melt. Furthermore, all the plasticisers studied in our work showed a good experimental solubility in the acrylic copolymer EUDRAGIT RS, thus resulting in homogeneous solid solutions by the application of the ram extruder.

However, as one could already mention within the qualitative comparison of the Hansen parameters in Table 1 and Figure 3, there exists a limit of solubility of plasticisers like DBS in the polymer matrix (at weight percentage of 19%). This could be proved by the DSC measurements of matrices containing 21.5% of DBS; a representative plot is presented in Figure 8. In contrast to homogeneous polymer/plasticiser blends where an amorphous step in the heat flow versus temperature plot is visible, a dent – marking the melting point of the plasticiser DBS – occurs on the plot. Therefore, this mixture actually existed of two different, only mechanically mixed, phases: a polymer and a plasticiser phase.

IBU exhibited a similar behaviour like the three plasticisers: again, a linear correlation of the weight proportion of IBU and the T_g of the matrix was found as it was also reported by Kidokoro et al. [34] that its ability to plasticise EUDRAGIT RS was slightly lower, compared with the plasticisers.

Table 4. Composition and experimental T_g values of all samples produced by hot-melt extrusion.

Polymer (%)	TEC (%)	ATBC (%)	DBS (%)	IBU (%)	T_g (K)	SD
100					336.7	0.6
89	11				305.3	0.9
85	15				300.9	1.2
78	22				280.4	1.1
90		10			310.0	0.6
86		14			303.9	1.4
79		21			289.7	0.9
91			9		304.6	0.5
85			15		296.1	0.5
81			19		285.0	1.7
90				10	318.5	0.3
80				20	300.5	0.9

By contrast, theophylline did neither influence the glass transition temperature of the pure polymer nor of the investigated polymer/plasticiser mixtures, which is in good agreement with previous works [30,34].

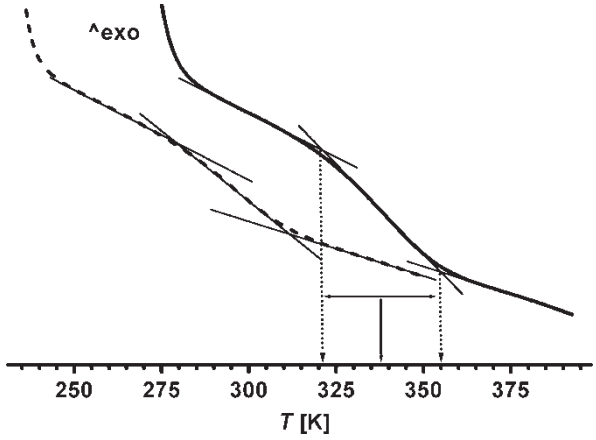

Figure 7. Plot of the heat flow against temperature T in a DSC experiment of a pure polymer (solid line) as well as a polymer–TEC mixture (dashed line) with $w = 17\%$. Both show a distinct step in the heat flow, marked by the onset/endset point with the midpoint between these two yielding the experimental value of the glass transition temperature T_g.

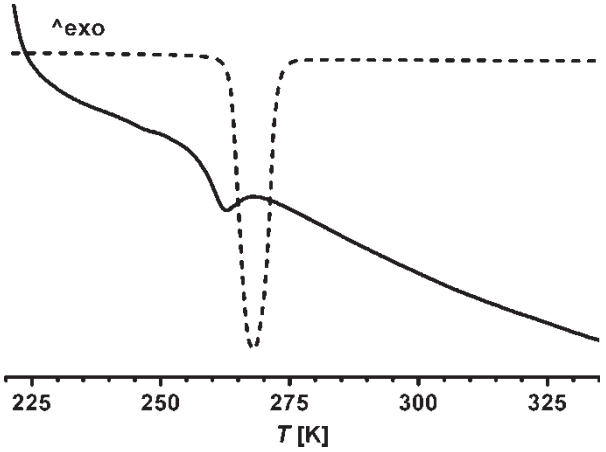

Figure 8. Plot of the heat flow against temperature T in a DSC experiment of a polymer–DBS mixture (solid line) with $w = 21.5\%$, as well as of pure DBS (dashed line). The melting peak of DBS is also visible in the polymer–DBS curve, thus indicating the existence of two different phases.

4. Conclusion

Our study shows that solubility properties of different polymer–plasticiser/drug blends can be calculated by the application of MD simulations using a proper force field. However, Hildebrand's parameter δ leads to an incomplete picture of the solubility property of a given system, e.g. polymer–DBS; although this lipophilic plasticiser exhibited nearly the same solubility parameter δ as the polymer (indicating a nearly ideal mixture), it showed an experimental solubility limit at higher plasticiser fractions. By contrast, solubility parameters, according to Hansen, deliver a more detailed picture by splitting δ in a dispersive δ_d and an electrostatic δ_e component: now, due to the large difference of δ_e between the polymer and the plasticiser, a solubility limit could be explained at least qualitatively.

However, a final decision as to whether a substance has the theoretical potential to build a stable blend with the polymer or not can only be made by calculating the Gibbs energy. As shown in Table 2, only TEC, ATBC, DBS and amorphous IBU showed a theoretical miscibility with the polymer. This was also proved by experiments studying hot-melt extrudates.

Based on these solubility calculations, only miscible polymer–plasticiser/drug systems were further investigated with respect to their plasticising properties. The correlation of the simulated T_g values with the experimental ones reflects the different solubility behaviours of the plasticisers studied: less miscible plasticisers like DBS and ATBC show a higher deviation from the experimental T_g values, while the good soluble plasticiser TEC, as well as the amorphous drug IBU, exhibits markedly less differences. Accordingly, it seems as if the modelling of the glass transition of polymer-like plasticisers results in a better agreement with experimental values compared with the less miscible substances. With the maximum discrepancies between simulated and experimental values being not more than 11% in the worst case, the validity of our improved computer model is demonstrated. Thus, it is possible to make predictions of the glass transition temperature of these systems with high precision.

As a concluding remark, it can be stated that our method gives pharmacists a valuable recipe of how to treat unknown polymer–plasticiser/drug systems with respect to their mixing and plasticising properties. The benefit of the presented method is a direct reduction of time expenditure and costs, in relation to the present trial and error principle in dosage form development.

References

[1] F.J.J. Leusen, S. Wilke, P. Verwer, and G.E. Engel, *Computational approaches to crystal structure and polymorph prediction*, in *Implications of Molecular and Materials Structure for New Technologies*, Vol. 360, NATO Science Series E, 1999, pp. 303–314.

[2] P. Verwer and F.J.J. Leusen, *Computer simulation to predict possible crystal polymorphs*, Rev. Comput. Chem. 12 (1998), pp. 327–365.

[3] L. Lawtrakul, H. Viernstein, and K. Wolschann, *Molecular dynamics simulations of β-cyclodextrin in aqueous solution*, Int. J. Pharm. 256 (2003), pp. 33–41.

[4] H. Viernstein, P. Weiss-Greiler, and K. Wolschann, *Quantitative determination of water in y-cyclodextrin by near-infrared spectroscopy*, Pharm. Ind. 67 (2005), pp. 122–125.

[5] K. Zhang and C.W. Manke, *Simulation of polymer solutions by dissipative particle dynamics*, Mol. Simul. 25(3/4) (2000), pp. 157–166.

[6] M. Meunier, *Diffusion coefficients of small gas molecules in amorphous cis-1,4-polybutadiene estimated by molecular dynamics simulations*, J. Chem. Phys. 123(13) (2005), 134906.

[7] Y. Aray, M. Marquez, J. Rodriguez, S. Coll, Y. Simón-Manso, C. Gonzalez, and D.A. Weitz, *Electrostatics for exploring the nature of water adsorption on the laponite sheets' surface*, J. Phys. Chem. B 107 (2003), pp. 8946–8952.

[8] M. Swenson, M. Languell, and J. Golden, *Modeling and simulation: The return on investment in materials science*, IDC White Paper (2004), pp. 1–24.

[9] A. Forster, J. Hempenstall, I. Tucker, and T. Rades, *Selection of excipients for melt extrusion with two poorly water-soluble drugs by solubility parameter calculation and thermal analysis*, Int. J. Pharm. 226(1–2) (2001), pp. 147–161.

[10] J.H. Hildebrand, *Solubility*, J. Am. Chem. Soc. 38(8) (1916), pp. 1452–1473.

[11] C.M. Hansen, *Hansen Solubility Parameters, A User's Handbook*, CRC Press, Boca Raton, 2000.

[12] J. Burke, *Solubility parameters: Theory and application*, in *AIC Book and Paper Group Annual*, Vol. 3, 1984, pp. 13–58. Available at http://aic.stanford.edu/sg/bpg/annual/v03/bp03-04.html (accessed 06/27/2006).

[13] P. Choi, *Molecular dynamics studies of the thermodynamics of HDPE/butene-based LLDPE blends*, Polymer 41(24) (2000), pp. 8741–8747.

[14] J. Han, R.H. Gee, and R.H. Boyd, *Glass transition temperatures of polymers from molecular dynamics simulations*, Macromolecules 27(26) (1994), pp. 7781–7784.

[15] L. Zhao and P. Choi, *Study of the correctness of the solubility parameters obtained from indirect methods by molecular dynamics simulation*, Polymer 45(4) (2004), pp. 1349–1356.

[16] M. Belmares, M. Blanco, W.A. Goddard III, R.B. Ross, G. Caldwell, S.H. Chou, J. Pham, P.M. Olofson, and C. Thomas, *Hildebrand and Hansen solubility parameters from molecular dynamics with applications to electronic nose polymer sensors*, J. Comput. Chem. 25(15) (2004), pp. 1814–1826.

[17] P. Choi, T.A. Kavassalis, and A. Rudin, *Estimation of the three-dimensional solubility parameters of alkyl phenol ethoxylates using molecular dynamics*, J Colloid Interface Sci. 150(2) (1992), pp. 386–393.

[18] T.A. Kavassalis, P. Choi, and A. Rudin, *The calculation of 3D solubility parameters using molecular models*, Mol. Simul. 11(2–4) (1993), pp. 229–241.

[19] H. Yang, L. Ze-Sheng, H. Qian, Y. Yang, X. Zhang, and C. Sun, *Molecular dynamics simulation studies of binary blend miscibility of poly(3-hydroxybutyrate) and poly(ethylene oxide)*, Polymer 45(2) (2004), pp. 453–457.

[20] Y. Zhu, N.H. Shah, A.W. Malick, M.H. Infeld, and J.W. McGinity, *Solid-state plasticization of an acrylic polymer with chlorpheniramine maleate and triethyl citrate*, Int. J. Pharm. 241(2) (2002), pp. 301–310.

[21] R. Gruetzmann and K.G. Wagner, *Quantification of the leaching of triethyl citrate/polysorbate 80 mixtures from Eudragit RS films by differential scanning calorimetry*, Eur. J. Pharm. Biopharm. 60(1) (2005), pp. 159–162.

[22] C.F. Fan, T. Cagin, W. Shi, and K.A. Smith, *Local chain dynamics of a model polycarbonate near glass transition temperature. A molecular dynamics simulation*, Macromol. Theory Simul. 6(1) (1997), pp. 83–102.

[23] K. Yu, Z. Li, and J. Sun, *Polymer structures and glass transition: A molecular dynamics simulation study*, Macromol. Theory Simul. 10(6) (2001), pp. 624–633.

[24] J.R. Fried and P. Ren, *Molecular simulation of the glass transition of polyphosphazenes*, Comput. Theor. Polym. Sci. 9(2) (1999), pp. 111–116.
[25] F.A. Momany and J.L. Willett, *Molecular dynamics calculations on amylose fragments. I. Glass transition temperatures of malto-decaose at 1, 5, 10 and 15.8% hydration*, Biopolymers 63(2) (2002), pp. 99–110.
[26] R. Roe, *MD Simulation study of glass transition and short time dynamics in polymer liquids*, in *Advances in Polymer Science, vol. 116*, L. Monnerie and U.W. Suter, eds., Springer, Berlin/Heidelberg, 1994, pp. 111–144.
[27] K.G. Wagner, M. Maus, A. Kornherr, and G. Zifferer, *Glass transition temperature of a cationic polymethacrylate dependent on the plasticizer content – Simulation vs. experiment*, Chem. Phys. Lett. 406 (2005), pp. 90–94.
[28] Y. Tamai, *A practical method to determine glass transition temperature in molecular dynamics simulation of mixed ionic glasses*, Chem. Phys. Lett. 351(1–2) (2002), pp. 99–104.
[29] S. Yoshioka, Y. Aso, and S. Kojima, *Prediction of glass transition temperature of freeze-dried formulations by molecular dynamics simulation*, Pharm. Res. 20(6) (2003), pp. 873–878.
[30] C. Wu and J.W. McGinity, *Non-traditional plasticization of polymeric films*, Int. J. Pharm. 177 (1999), pp. 15–27.
[31] J. Siepmann, F. Lecomte, and R. Bodmeier, *Diffusion-controlled drug delivery systems: Calculation of the required composition to achieve desired release profiles*, J. Control. Release 60(2–3) (1999), pp. 379–389.
[32] H. Rey, K.G. Wagner, P. Wehrle, and P.C. Schmidt, *Development of matrix-based theophylline sustained-release microtablets*, Drug Dev. Ind. Pharm. 26(1) (2000), pp. 21–26.
[33] S. Narisawa, M. Nagata, C. Danyoshi, H. Yoshino, K. Murata, Y. Hirakawa, and K. Noda, *An organic acid-induced sigmoidal release system for oral controlled-release preparations*, Pharm. Res. 11(1) (1994), pp. 111–116.
[34] M. Kidokoro, N.H. Sha, A.W. Malick, M.H. Infeld, and J.W. McGinity, *Properties of tablets containing granulations of ibuprofen and an acrylic copolymer prepared by thermal processes*, Pharm. Dev. Technol. 6(2) (2001), pp. 263–275.
[35] N. Follonier, E. Doelke, and E.T. Cole, *Evaluation of hot-melt extrusion as a new technique for the production of polymer-based pellets for sustained release capsules containing high loadings of freely soluble drugs*, Drug Dev. Ind. Pharm. 20(8) (1994), pp. 1323–1339.
[36] Y. Zhu, N.H. Shah, A.W. Malick, M.H. Infeld, and J.W. McGinity, *Influence of a lipophilic thermal lubricant on the processing conditions and drug release properties of chlorpheniramine maleate tablets prepared by hot-melt extrusion*, J. Drug Del. Sci. Technol. 14(4) (2004), pp. 313–318.
[37] H.C. Andersen, *Molecular dynamics simulations at constant pressure and/or temperature*, J. Chem. Phys. 72(4) (1980), pp. 2384–2393.
[38] M.J. Hwang, T.P. Stockfisch, and A.T. Hagler, *Derivation of class II force fields. 2. Derivation and characterization of a class II force field, CFF93, for the alkyl functional group and alkane molecules*, J. Am. Chem. Soc. 116(6) (1994), pp. 2515–2525.
[39] H. Sun, Ab initio *calculations and force field development for computer simulation of polysilanes*, Macromolecules 28(3) (1995), pp. 701–712.
[40] H. Sun, *COMPASS: An* ab initio *force-field optimized for condensed-phase applications-overview with details on alkane and benzene compounds*, J. Phys. Chem. B 102(38) (1998), pp. 7338–7364.
[41] S.W. Bunte and H. Sun, *Molecular modeling of energetic materials: The Parameterization and validation of nitrate esters in the COMPASS force field*, J. Phys. Chem. B 104(11) (2000), pp. 2477–2489.
[42] Y. Zhu, N.H. Shah, A.W. Malick, M.H. Infeld, and J.W. McGinity, *Influence of thermal processing on the properties of chlorpheniramine maleate tablets containing an acrylic polymer*, Pharm. Dev. Technol. 7(4) (2002), pp. 481–489.
[43] N. Schuld and B.A. Wolf, *Polymer-solvent interaction parameters*, in *Polymer Handbook*, J. Brandrup, E.H. Immergut, and E.A. Grulke, eds., Wiley, New York, 1999, pp. 675–688.
[44] T.A. Kavassalis, P. Choi, and A. Rudin, *Molecular models and three dimensional solubility parameters of non-ionic surfactants*, in *Molecular Simulation and Industrial Applications*, K.E. Gubbins and N. Quirke, eds., Gordon & Breach, Amsterdam, 1996, pp. 315–329.
[45] C. Wu and J.W. McGinity, *Influence of methylparaben as a solid-state plasticizer on the physicochemical properties of Eudragit RS PO hot-melt extrudates*, Eur. J. Pharm. Biopharm. 56 (2003), pp. 95–100.
[46] R. Chang and C. Hsiao, *Eudragit RL and RS pseudolatices: Properties and performance in pharmaceutical coating as a controlled release membrane for theophylline pellets*, Drug Dev. Ind. Pharm. 15(2) (1989), pp. 187–196.
[47] J.C. Gutiérrez-Rocca and J.W. McGinity, *Influence of water soluble and insoluble plasticizers on the physical and mechanical properties of acrylic resin copolymers*, Int. J. Pharm. 103(3) (1994), pp. 293–301.
[48] L.H. Sperling, *Introduction to Physical Polymer Science*, Wiley, New York, 2001, pp. 73–75.